Article:

Mitseas, I.P. orcid.org/0000-0001-5219-1804, Zhang, Y. and Fragkoulis, V.C. orcid.org/0000-0001-9925-9167 (2025) Risk assessment of block random rocking on nonlinear foundation subject to evolutionary seismic ground motion. Mechanical Systems and Signal Processing, 240. 113397. ISSN: 0888-3270

https://doi.org/10.1016/j.ymssp.2025.113397

Risk assessment of block random rocking on nonlinear foundation subject to evolutionary seismic ground motion

Ioannis P. Mitseas[a,b], Yuanjin Zhang[c,*], Vasileios C. Fragkoulis[d]

[a] *School of Civil Engineering, University of Leeds, Leeds, LS2 9JT, UK*
[b] *School of Civil Engineering, National Technical University of Athens, Iroon Polytechneiou 9, Zografou, Athens, 15780, Greece*
[c] *School of Safety Science and Emergency Management, Wuhan University of Technology, Wuhan, 430070, China*
[d] *Department of Civil and Environmental Engineering, University of Liverpool, Liverpool, L69 3GH, UK*

Abstract

This study develops an approximate semi-analytical framework for assessing the toppling survival probability of a rigid block subject to stochastic seismic excitation defined in accordance with modern aseismic codes provisions. The rocking system incorporates a nonlinear flexible foundation model that allows for uplifting and nonlinear damping, reflecting realistic soil-structure interaction effects. A nonlinear contact force of the Hunt and Crossley's kind is employed. Using a stochastic averaging approach, the proposed method accounts for the unbounded response behavior associated with toppling, paralleling challenges observed in systems with negative stiffness. The nonstationary probability density function (PDF) of the rocking amplitude is formulated to quantify the survival

*email@corresponding.author
Email address: ylzhyj@whut.edu.cn (Yuanjin Zhang)

probability over time efficiently. This technique offers significant computational advantages over traditional numerical simulations while capturing the effects of time-dependent excitation intensity and frequency content. Numerical examples, including rigid blocks rocking on various nonlinear flexible foundations under evolutionary seismic excitations, validate the proposed framework. Comparisons with Monte Carlo simulations confirm the accuracy and reliability of the method, emphasizing its utility for probabilistic assessment in seismic engineering contexts.
Keywords: Rocking motion, Nonlinear flexible foundation, Random base excitation, Stochastic averaging, Uplifting, Toppling probability

1. Introduction

The rocking of rigid structures has long been a topic of critical interest in earthquake engineering, ever since the foundational work of Housner [1] demonstrated the unexpectedly stable dynamic behavior of free-standing, slender bodies under seismic loading. Two principal modeling approaches have historically underpinned the study of such systems: the Housner Model (HM), which represents a rigid block rocking on a rigid foundation, and the Winkler Foundation Model (WFM), which simulates the interaction with an elastic foundation using discrete spring elements [2–6]. These models have served as the analytical basis for capturing the inherently nonlinear and discontinuous dynamics of rocking responses.

Rocking provides a natural mechanism for seismic energy dissipation through uplift and impact, effectively decoupling lateral inertial demands from internal deformation and thus reducing the likelihood of structural damage. A major benefit of enabling uplift is the avoidance of cyclic degradation typically observed in conventional plastic hinge mechanisms. In this setting, energy is dissipated via repeated impacts, while the structure's integrity is preserved. Uplift allows structural elements to temporarily detach from their base, resulting in large but recoverable displacements that reduce peak seismic demand, limit residual deformation, and enable self-centering behavior. As such, rocking is increasingly adopted not only as a survival mechanism but also as a deliberate strategy in modern resilience-oriented seismic design [7]. These advantages have fueled strong and growing interest from the engineering community in this field. Recent research has expanded this paradigm through the development of controlled rocking systems, including rocking shear walls and externally dissipative pinned braced frames, which promote uniform interstory drift, minimize residual displacements, and activate lower-hierarchy failure mechanisms, thus reducing the risk of soft-story collapse and improving seismic performance [8]. Additional fields of application include the seismic protection of small-scale or sensitive installations, such as museum exhibits, marble heritage monuments [9], and critical machinery [10, 11] in medical or military facilities, where both structural integrity and operational continuity are essential. Despite the advancements, block-like systems rocking on nonlinear flexible foundations have received comparatively less attention, particularly under stochastic seismic excitation [12], although there is a body of research in the case of stationary excitation and pulse-like ground motion (e.g., [7, 13, 14]). To address this, the present study introduces a stochastic semi-analytical framework that combines static condensation, statistical linearization, and stochastic averaging to evaluate the survival probability [15, 16]–defined as the probability of avoiding toppling–of a rigid block subjected to nonstationary, Eurocode 8 (EC8)-compatible excitation. The formulation captures the nonlinearities of the block–foundation interaction, including uplift effects and negative stiffness phases, and fully incorporates the evolutionary nature of realistic seismic input [17], enabling a more accurate and analytically tractable representation of the problem. This approach is particularly well-suited for performance-based analysis and risk-informed decision-making [18, 19].

The proposed framework offers a novel contribution by evaluating the survival probability of rocking block systems under nonstationary seismic loading. Unlike prior approaches that neglect the possibility of unbounded responses when the foundation stiffness becomes negative, the present method accounts for this through a specially formulated nonstationary response amplitude probability density function (PDF). A key advantage of the approach is its ability to accommodate stochastic excitations that vary in both intensity and frequency content—thus reflecting the nonstationary and multi-scale nature of seismic ground motions.

In the remainder of this paper, Sections 2.1 through 2.3 lay out the mathematical foundations that form the basis of the proposed semi-analytical framework. Section 2.4 delves into the mechanization of the proposed technique. Subsequently, Sections 3.1 to 3.3 present representative case studies that illustrate the application of the proposed stochastic dynamics framework to rigid blocks of different geometries rocking on various nonlinear flexible foundations, subjected to seismic excitations modeled through EC8 elastic design spectra. The accuracy and reliability of the proposed approach is rigorously evaluated through a comparative analysis against Monte Carlo simulation (MCS) data obtained from nonlinear response history analysis (RHA). Lastly, Section 4 synthesizes the key findings and offers concluding remarks on the broader implications of the study.

2. Mathematical formulation

This section articulates the mathematical formulation underlying the proposed methodology for efficiently assessing the survival probability of randomly excited rocking rigid blocks. Emphasis is placed on clearly delineating the key assumptions and simplifications introduced to balance analytical rigor with computational tractability. To preserve coherence and enhance the manuscript's readability, only the essential theoretical constructs related to the generation of response spectrum-compatible stochastic processes are presented herein, while a more detailed exposition is deferred to the Appendix A. The specific EC8 elastic design spectra employed in the analysis are provided in the Appendix B.

2.1. Block random rocking on nonlinear flexible foundation modeling

In this section, the modeling of a rectangular rigid block on nonlinear flexible foundation is briefly reviewed following the foundational approaches presented in Refs. [20, 21]. The coupled equations governing the dynamics of a quiescent rectangular rigid block rocking on nonlinear foundation subjected to base excitation modeled as a nonstationary stochastic seismic acceleration process are given by

$$m\ddot{z}_{zb} + mh(\dot{\theta}^2 \cos\theta + \ddot{\theta}\sin\theta) + F_{cb} - mg = m\ddot{z}_g \tag{1}$$

and

$$(I_{cm} + mh^2)\ddot{\theta} + M_{cb} + mh(\ddot{z}_{cb} - g)\sin\theta = mh(\ddot{x}_g \cos\theta - \ddot{z}_g \sin\theta), \tag{2}$$

where m, $2h$ and I_{cm} denote the mass, height, and polar moment of inertia around the center of mass of the rectangular rigid block, respectively; $z_{cb}(t)$ and $\theta(t)$ represent the vertical displacement of the base center cb and the rotation angle of the block; and $\ddot{z}_x(t)$ and $\ddot{z}_g(t)$ are the horizontal and vertical induced accelerations of nonstationary stochastic processes, respectively. Note that $\ddot{z}_x(t)$ and $\ddot{z}_g(t)$ can be defined as possessing evolutionary power spectra (EPS) $G_h(\omega, \zeta_0, t; a_g^s)$ and $G_v(\omega, \zeta_0, t; a_g^s)$ compatible with a target pseudo-acceleration response spectrum $S(\omega, \zeta_0; a_g^s)$, where ζ_0 denotes the damping ratio of the corresponding linear oscillator, ω represents the frequency and a_g^s is the scaled images of the seismic excitation intensity.

In the nonlinear, coupled and piecewise Eqs. (1) and (2), g denotes the gravity acceleration, while F_{cb} and M_{cb} are the vertical force and moment of the contact force with respect to the center of base, respectively. The latter are related to the nature of the impact force [3, 20, 22]. Considering Hunt and Crossley's model [23], used in several studies [24–26], and accounting for the uplift of the base corners above the ground level, F_{cb} and M_{cb} can be described as

$$F_{cb} = 2bkz_{cb} + 2b\lambda z_{cb}\dot{z}_{cb} + \frac{2}{3}b^3\lambda\dot{\theta}\sin\theta\cos\theta \tag{3}$$

and

$$M_{cb} = \frac{2}{3}b^3k\sin\theta\cos\theta + \frac{2}{3}b^3\lambda\dot{z}_{cb}\sin\theta\cos\theta + \frac{2}{3}b^3\lambda z_{cb}\dot{\theta}\cos^2\theta, \tag{4}$$

for the case of no-uplifting and

$$\begin{aligned} F_{cb} =& \frac{1}{2}b^2k\sin\theta\mathrm{sgn}\theta + kz_{cb}\left(b + \frac{1}{2}\frac{z_{cb}}{\sin\theta}\mathrm{sgn}\theta\right) + \frac{1}{2}b^2\lambda\dot{z}_{cb}\sin\theta\mathrm{sgn}\theta \\ &+ \lambda z_{cb}\dot{z}_{cb}\left(b + \frac{1}{2}\frac{z_{cb}}{\sin\theta}\mathrm{sgn}\theta\right) + \frac{1}{3}b^3\lambda\dot{\theta}\sin\theta\cos\theta \\ &+ \frac{1}{2}\lambda z_{cb}\dot{\theta}\cos\theta\left(b^2 - \frac{1}{3}\frac{z_{cb}^2}{\sin^2\theta}\right)\mathrm{sgn}\theta \end{aligned} \tag{5}$$

and

$$\begin{aligned} M_{cb} =& \frac{1}{3}b^3k\sin\theta\cos\theta + \frac{1}{2}kz_{cb}\cos\theta\left(b^2 - \frac{1}{3}\frac{z_{cb}^2}{\sin^2\theta}\right)\mathrm{sgn}\theta + \frac{1}{3}b^3\lambda\dot{z}_{cb}\sin\theta\cos\theta \\ &+ \frac{1}{4}b^4\lambda\dot{\theta}\sin\theta\cos^2\theta\mathrm{sgn}\theta + \frac{1}{2}\lambda z_{cb}\dot{z}_{cb}\cos\theta\left(b^2 - \frac{1}{3}\frac{z_{cb}^2}{\sin^2\theta}\right)\mathrm{sgn}\theta \\ &+ \frac{1}{3}\lambda z_{cb}\dot{\theta}\cos^2\theta\left(b^3 + \frac{1}{4}\frac{z_{cb}^3}{\sin^3\theta}\mathrm{sgn}\theta\right) \end{aligned} \tag{6}$$

for the uplifting case. Accordingly, two distinct states are identified. The first corresponds to the no-uplift state, which prevails as long as the entire base of the block remains in full contact with the ground. In contrast, the uplift state arises when either of the pivot points lifts off the ground surface. The two distinct states are illustrated in Figs. 1(a) and 1(b), respectively. In Eqs. (3) to (6), b represents half of the width of the rigid block, $\mathrm{sgn}(\cdot)$ is the signum function, and k (force units per unit width of base per unit vertical deformation) and λ (force units per unit width of base per unit vertical deformation velocity and per unit vertical deformation) denote the stiffness and damping coefficients of the impact force model, respectively.

Since θ and z_{cb} are typically small in most practical applications (e.g., [3, 20]), reasonable approximations can be obtained by assuming $\sin\theta \approx 0$ and $\cos\theta \approx 1$. Further simplification can be introduced by neglecting combined derivative order terms of θ and z_{cb} that are greater than one. Subsequently, considering the static condensation method yields [21]

$$z_{cb} = z_{st} = \frac{mg}{2bk} \tag{7}$$

for the case of no-uplifting, and

$$z_{cb} = z_{st} = \frac{-bk\theta\mathrm{sgn}\theta + \sqrt{2mgk\theta\mathrm{sgn}\theta}}{2k} \tag{8}$$

for the case of uplifting. Clearly, in this manner, the uplifting occurs when $|\theta| > \theta_{ul}$ with

$$\theta_{ul} = \frac{|z_{st}|}{b} = \frac{mg}{2b^2k}. \tag{9}$$

Substituting Eqs. (3) to (8) into Eqs. (1) and (2), while accounting for the horizontal component of the induced excitation, i.e., $\ddot{z}_g = 0$, the rocking motion of the

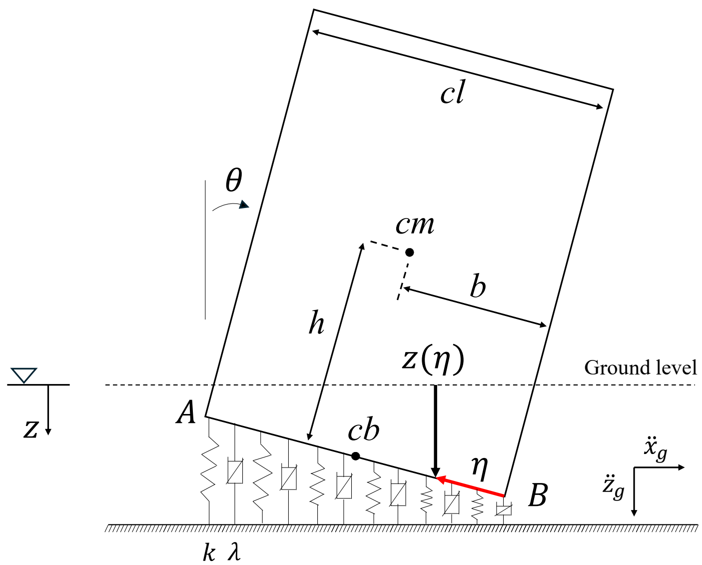

(a)

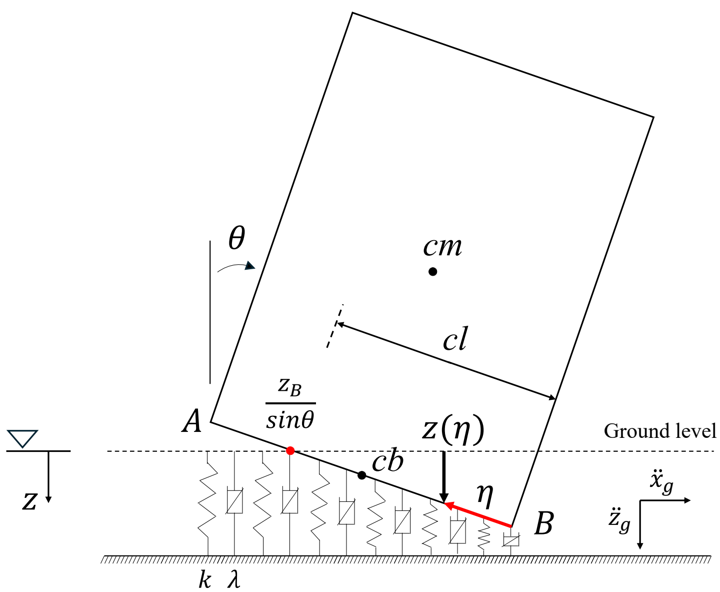

(b)

Fig. 1. Block rocking on nonlinear flexible foundation: (a) no-uplifting with $\theta > 0$; (b) uplifting with $\theta > 0$. Definition of the contact line (cl) for each case. The system exhibits an analogous behavior in both states for $\theta < 0$.

rectangular rigid block can be cast into the form

$$\ddot{\theta} + \frac{C(\theta)}{m_{sdof}}\dot{\theta} + \frac{K(\theta)}{m_{sdof}}\theta = \frac{mh}{m_{sdof}}\ddot{x}_g, \tag{10}$$

where

$$m_{sdof} = I_{cm} + mh^2, \tag{11}$$

$$C(\theta) = \begin{cases} \frac{b^2}{3}\lambda\frac{mg}{k}, & |\theta| \leq \theta_{ul} \\ \frac{mgb\lambda}{6k^2}\frac{\sqrt{2mgk\theta\text{sgn}\theta}}{\theta}\text{sgn}\theta, & |\theta| > \theta_{ul} \end{cases} \tag{12}$$

and

$$K(\theta) = \begin{cases} \frac{2b^3}{3}k - mgh, & |\theta| \leq \theta_{ul} \\ mg\left(\frac{b\text{sgn}\theta}{\theta} - \frac{\sqrt{2mgk\theta\text{sgn}\theta}}{3k\theta^2} - h\right), & |\theta| > \theta_{ul} \end{cases} \tag{13}$$

2.2. Stochastic averaging and linearization treatment

It is important to note that the stiffness coefficient $K(\theta)$ in Eq. (13) can become zero or even negative for certain combinations of system parameters. A negative stiffness promotes toppling behavior, whereas a positive stiffness tends to restore the system to its original position. Therefore, a special treatment combining stochastic averaging and linearization methods is adopted in this section to determine the rocking response of the rigid block under evolutionary nonstationary stochastic excitation [16, 27].

In this context, considering that the stochastic excitation is slowly varying with respect to time and also that the system is lightly damped, it is assumed that the system exhibits a pseudo-harmonic behavior (e.g., [28]) under the nonoverturning condition. Therefore, the rotation angle satisfies

$$\theta(t) = a\cos[\omega(a)t + \phi(t)], \tag{14}$$

where a and ϕ denote the slowly time-varying amplitude and phase, respectively. To further simplify the ensuing analysis, Eq. (10) can be rewritten as

$$\ddot{\theta} + \beta_0\theta + z(t,\theta,\dot{\theta}) = \frac{mh}{m_{sdof}}\ddot{x}_g, \tag{15}$$

where β_0 is the damping coefficient of the corresponding linear system, and

$$z(t,\theta,\dot{\theta}) = \frac{C(\theta)}{m_{sdof}}\dot{\theta} + \frac{K(\theta)}{m_{sdof}}\theta - \beta_0\theta. \tag{16}$$

Applying next the statistical linearization method [29], an equivalent amplitude-dependent linear system is defined as

$$\ddot{\theta} + \beta(a)\dot{\theta} + \omega^2(a)\theta = \frac{mh}{m_{sdof}}\ddot{x}_g, \tag{17}$$

where $\beta(a)$ and $\omega^2(a)$ represent, respectively, the equivalent amplitude-dependent damping and stiffness elements. The latter are determined following a mean-square minimization of the difference between Eqs. (15) and (17) (e.g., [27, 29, 30]), and are given by

$$\beta(a) = \beta_0 - \frac{1}{a\omega(a)\pi}\int_0^{2\pi} \sin\varphi \cdot z\left(t, a\cos\varphi, -a\omega(a)\sin\varphi\right)\mathrm{d}\varphi \tag{18}$$

and

$$\omega^2(a) = \frac{1}{a\pi}\int_0^{2\pi} \cos\varphi \cdot z(t, a\cos\varphi, -a\omega(a)\sin\varphi)\mathrm{d}\varphi, \tag{19}$$

with $\varphi = \omega(a)t + \phi(t)$. Substituting Eq. (16) into Eqs. (18) and (19) yields

$$\beta(a) = \begin{cases} \dfrac{b^2\lambda mg}{3km_{sdof}}, & a \le \theta_{ul} \\ \dfrac{4mgb\lambda}{3\pi k^2 m_{sdof}}\sqrt{\dfrac{2mgk}{a}}\{{}_2F_1([-0.5, 0.25]; 1.25; 1) \\ \qquad - \sqrt{\cos y}\ {}_2F_1([-0.5, 0.25]; 1.25; \cos^2 y)\} \\ \qquad - \dfrac{4b^2\lambda mg}{3\pi km_{sdof}}\left(\dfrac{\pi}{4} - \dfrac{y}{2} - \dfrac{\sin 2y}{4}\right), & a > \theta_{ul} \end{cases} \tag{20}$$

and

$$\omega^2(a) = \begin{cases} \dfrac{2b^3k}{3m_{sdof}} - \dfrac{mgh}{m_{sdof}}, & a \le \theta_{ul} \\ \dfrac{4}{\pi m_{sdof}}\left\{\dfrac{mgb\sin y}{a} - \dfrac{2mg}{3ka}\sqrt{\dfrac{2mgk}{a}}E\left(\dfrac{y}{2}, 2\right) - mgh\left(\dfrac{y}{2} + \dfrac{\sin 2y}{4}\right)\right. \\ \qquad \left. + \left(\dfrac{2b^2\lambda}{3} - mgh\right)\left(\dfrac{\pi}{4} - \dfrac{y}{2} - \dfrac{\sin 2y}{4}\right)\right\}, & a > \theta_{ul} \end{cases} \tag{21}$$

where $y = \arccos\left(\dfrac{\theta_{ul}}{a}\right)$. In Eq. (20), ${}_2F_1(\cdot)$ denotes the generalized hypergeometric function, while in Eq. (21) $E(\cdot)$ represents the incomplete elliptic integral of the second kind. These are given by

$$_2F_1([a_1, a_2]; b_1; z) = \sum_{n=0}^{\infty}\left(\frac{(a_1)_n(a_2)_n}{(b_1)_n(a_2)_n}\right)\left(\frac{z^n}{n!}\right) \tag{22}$$

and

$$E\left(\lambda, \rho\right) = \int_0^{\lambda} \sqrt{1 - \rho \sin^2 \varphi} \mathrm{d}\varphi, \tag{23}$$

where $(\cdot)_n$ is the Pochhammer symbol, defined as

$$(a)_n = \frac{\Gamma(a+n)}{\Gamma(a)}, \tag{24}$$

and $\Gamma(\cdot)$ is the complete Gamma function provided as

$$\Gamma(a) = \int_0^{\infty} t^{a-1} e^{-t} \mathrm{d}t. \tag{25}$$

To further simplify the analysis, the amplitude-dependent equivalent elements in Eq. (17) are approximated by corresponding time-dependent ones [27, 29, 31], defined as the nonstationary mean values of the former. Therefore, Eq. (17) becomes

$$\ddot{\theta} + \beta_{eq}(t)\theta + \omega_{eq}^2(t)\theta = \frac{mh}{m_{sdof}} \ddot{x}_g, \tag{26}$$

where the time-dependent damping $\beta_{eq}(t)$ and stiffness $\omega_{eq}^2(t)$ elements are given by

$$\beta_{eq}(t) = \int_0^{\infty} \beta(a) p(a,t) \mathrm{d}t \tag{27}$$

and

$$\omega_{eq}^2(t) = \int_0^{\infty} \omega^2(a) p(a,t) \mathrm{d}t. \tag{28}$$

Based on the nature of the nonstationary rocking response amplitude PDF $p(a,t)$, the time-dependent stiffness element $\omega_{eq}^2(t)$ comprises two parts: the bounded part

$\omega^2_{eq,B}(t)$ for $a \in [0, a_{cr}]$, and the unbounded part for $a \in (a_{cr}, \infty)$, which may lead to toppling. In this context, the bounded equivalent damping element is expressed as

$$\beta_{eq,B}(t) = \int_0^{a_{cr}} \beta(a)p(a,t)\mathrm{d}t, \tag{29}$$

while the corresponding bounded equivalent stiffness is given by

$$\omega^2_{eq,B}(t) = \int_0^{a_{cr}} \omega^2(a)p(a,t)\mathrm{d}t, \tag{30}$$

where $p(a,t)$ denotes the nonstationary response amplitude PDF. Expanding on Eq. (21), it is clear that the equivalent stiffness element will become zero when the rocking amplitude reaches a critical value a_{cr}. In this context, considering that the system exhibits an unbounded response when $a > a_{cr}$, a special form of nonstationary rocking amplitude PDF is adopted [16]. Specifically, this is

$$p(a,t) = \frac{a}{c(t)} \exp\left(-\frac{a^2}{2c(t)}\right)\mathrm{rect}(a) + \exp\left(-\frac{a^2_{cr}}{2c(t)}\right)\delta(a - a_\infty), \tag{31}$$

where $\mathrm{rect}(a) = u(a) - u(a - a_{cr})$, with $u(\cdot)$ denoting the unit step function, $c(t)$ is a coefficient to be determined, and $\delta(\cdot)$ is the Dirac delta function. A detailed discussion about the proposed nonstationary response amplitude PDF $p(a,t)$ in Eq. (31) can be found in [16, 32].

Furthermore, for $a \in [0, a_{cr}]$, the stochastic averaging method is employed

[33, 34], resulting in the following Fokker-Planck (F-P) differential equation

$$\frac{\partial p(a,t|a_1,t_1)}{\partial t} = -\frac{\partial}{\partial a}\left[\left(-\frac{1}{2}\beta_{eq,B}(t)a + \frac{\pi S_h(\omega_{eq,B}(t),\zeta_0,t;a_g^s)}{2a\omega_{eq,B}^2(t)}\right)p(a,t|a_1,t_1)\right] + \frac{1}{2}\frac{\partial^2}{\partial a^2}\left[\frac{\pi S_h(\omega_{eq,B}(t),\zeta_0,t;a_g^s)}{\omega_{eq,B}^2(t)}p(a,t|a_1,t_1)\right], \tag{32}$$

where $S_h(\omega_{eq,B}(t),\zeta_0,t;a_g^s) = \left(\frac{mh}{m_{sdof}}\right)^2 G_h(\omega_{eq,B}(t),\zeta_0,t;a_g^s)$. It is readily seen that the truncated Rayleigh PDF part of Eq. (31) satisfies the bounded F-P Eq. (32) when $a_1 = 0$ and $t_1 = 0$. Thus, substituting the truncated Rayleigh PDF into Eq. (32), the following nonlinear differential equation can be obtained

$$\dot{c}(t) = -\beta_{eq,B}(t)c(t) + \frac{\pi S_h(\omega_{eq,B}(t),\zeta_0,t;a_g^s)}{\omega_{eq,B}^2(t)}. \tag{33}$$

Moreover, the transitional amplitude PDF $p(a,t|a_1,t_1)$ can be derived in the form

$$p(a,t|a_1,t_1) = \begin{cases} p_{tr}(a,t|a_1,t_1) + R(t,t_1)\delta(a-a_\infty), & 0 \leq a_1 \leq a_{cr} \\ \delta(a-a_\infty), & a_1 > a_{cr} \end{cases} \tag{34}$$

where

$$p_{tr}(a,t|a_1,t_1) = \frac{a}{c(t,t_1)}\exp\left[-\frac{a^2+h^2(t,t_1)}{2c(t,t_1)}\right] I_0\left[\frac{ah(t,t_1)}{c(t,t_1)}\right]\text{rect}(a) \tag{35}$$

corresponds to the component for rocking amplitude lower than the critical value

a_{cr}, and δ is the Dirac delta function. Further,

$$R(t, t_1) = 1 - \int_0^{a_{cr}} p_{tr}(a, t|a_1, t_1)\mathrm{d}a \tag{36}$$

and $I_0(\cdot)$ denotes the modified Bessel function of the first kind and of zero order. In Eq. (35), $c(t, t_1)$ and $h(t, t_1)$ satisfy

$$\frac{\mathrm{d}c(t, t_1)}{\mathrm{d}t} + \beta_{eq,B}(t)c(t, t_1) - \frac{\pi S_h(\omega_{eq,B}(t), \zeta_0, t; a_g^s)}{\omega_{eq,B}^2(t)} = 0 \tag{37}$$

and

$$\frac{\mathrm{d}h(t, t_1)}{\mathrm{d}t} + \frac{1}{2}\beta_{eq,B}(t)h(t, t_1) = 0, \tag{38}$$

subject to $p(a, t|a_1, t_1) = \delta(a - a_1)$. These are derived following a treatment similar to that in Ref. [35]; that is by substituting the bounded part of Eq. (35) into Eq. (32).

2.3. Block random rocking reliability assessment over toppling

In this section, the survival probability over toppling pertaining to a rigid block system rocking on nonlinear flexible foundation is considered. The survival probability in this case is defined as the probability $P_B(t)$ that the rocking amplitude a is kept below the specified threshold a_{cr} over the time duration $[0, T]$. By discretizing the time duration as $[0, T] = \bigcup_{i=1}^{M} [t_{i-1}, t_i]$, with $t_0 = 0$ and $t_M = T$, the survival probability is computed by [30, 36]

$$P_B(T = t_M) = \prod_{i=1}^{M} (1 - F_i), \tag{39}$$

where F_i denotes the probability that a crosses the barrier a_{cr} in the time interval $[t_{i-1}, t_i]$, while no crossing has occured prior to the time instant t_{i-1}. This is defined as

$$F_i = \frac{\text{Prob}[a(t_i) \geq a_{cr} \cap a(t_{i-1}) < a_{cr}]}{\text{Prob}[a(t_{i-1}) < a_{cr}]} = \frac{Q_{i-1,i}}{H_{i-1}}, \tag{40}$$

where

$$H_{i-1} = \int_0^{a_{cr}} p(a_{i-1}, t_{i-1}) \mathrm{d}a_{i-1} \tag{41}$$

and

$$Q_{i-1,i} = \int_{a_{cr}}^{\infty} \mathrm{d}a_i \int_0^{a_{cr}} p(a_{i-1}, t_{i-1}; a_i, t_i) \mathrm{d}a_{i-1}. \tag{42}$$

Substituting Eqs. (31) and (34) into Eqs. (41) and (42), and manipulating, yields [16, 30]

$$H_{i-1} = 1 - \exp\left[-\frac{a_{cr}^2}{2c(t_{i-1})}\right] \tag{43}$$

and

$$Q_{i-1,i} = H_{i-1} - \int_0^{a_{cr}} \mathrm{d}a_i \int_0^{a_{cr}} p_{tr}(a_{i-1}, t_{i-1}; a_i, t_i) \mathrm{d}a_{i-1}. \tag{44}$$

For the small time interval $[t_{i-1}, t_i]$, assuming the EPS is slowly varying with respect to time and adopting a first-order Taylor expansion, Eqs. (37) and (38) become

$$c(t_{i-1}, t_i) = \frac{\pi S_h(\omega_{eq,B}(t), \zeta_0, t; a_g^s)}{\omega_{eq,B}^2(t)}(t_i - t_{i-1}) \tag{45}$$

and

$$h(t_{i-1}, t_i) = a_{i-1}\sqrt{1 - \beta_{eq,B}(t)(t_i - t_{i-1})}, \tag{46}$$

respectively. Further, considering Eqs. (45) and (46), Eq. (44) takes the form

$$Q_{i-1,i} = (1 - r_i^2)\left\{1 - \exp\left[-\frac{a_{cr}^2}{2c(t_{i-1})(1 - r_i^2)}\right]\right\}\exp\left[\frac{a_{cr}^2}{2c(t_i)(1 - r_i^2)}\right] + \sum_{n=1}^{N} D_n, \tag{47}$$

where

$$D_n = \frac{r_i^{2n}(1 - r_i^2)}{(n!)^2}\Gamma\left[1 + n, \frac{a_{cr}^2}{2c(t_i)(1 - r_i^2)}\right] \times \left\{\Gamma[1 + n, 0] - \Gamma\left[1 + n, \frac{a_{cr}^2}{2c(t_{i-1})(1 - r_i^2)}\right]\right\}. \tag{48}$$

The parameter r_i^2 is given by

$$r_i^2 = \frac{c(t_{i-1})}{c(t_i)}\left(1 - \beta_{eq,B}(t_{i-1})\tau_i\right) \tag{49}$$

and can be interpreted as an indicator of the correlation between random variables a_{i-1} and a_i, since $r_i^2 \to 0$ as $\tau_i \to \infty$, and $r_i^2 \to 1$ as $\tau_i \to 0$ [30].

2.4. Mechanization of the proposed technique

The implementation of the approximate stochastic dynamics technique developed herein for assessing the survival probability over toppling of a rigid block rocking on a flexible nonlinear foundation, excited by an evolutionary stochastic process compatibly defined with contemporary seismic codes provisions (e.g., [37, 38]), involves the following steps:

i. Derive an excitation EPS characterizing the induced ground motion, following the specifications provided in Appendix B for a given elastic design spectrum; see Appendix A.

ii. Use a standard integration scheme to numerically solve the first-order differential Eq. (33) to determine the time-dependent coefficient $c(t)$.

iii. Utilize $c(t)$ in the previous step in conjunction with Eq. (31) and Eqs. (29) and (30) to compute the nonstationary response amplitude PDF $p(a, t)$, and the bounded equivalent linear elements, $\beta_{eq,B}(t)$ and $\omega^2_{eq,B}(t)$.

iv. Discretize the time domain as discussed in Section 2.3. Specifically,

$$[t_{i-1}, t_i], \quad i = 1, 2, \ldots, M, \quad t_i = t_{i-1} + d_T T_{\text{eq,B}}(t_{i-1}), \tag{50}$$

where T_{eq} is the equivalent natural period of the rocking block, $T_{\text{eq,B}}(t) = \frac{2\pi}{\omega_{\text{eq,B}}(t)}$, and d_T is a selected constant in $(0, 1]$.

v. Employ Eqs. (43) and (47) for the computation of the H_{i-1} and Q_{i-1}, respectively.

vi. Substitute H_{i-1} and Q_{i-1} of the previous step into Eq. (39) to compute the survival probability P_B over toppling.

3. Numerical case studies

In this section, the proposed framework is verified by considering the cases of rigid blocks rocking on various flexible nonlinear foundations excited by evolutionary stochastic processes compatible with contemporary aseismic codes (e.g., [37, 38]). The EC8 design spectrum for soil type B detailed in Appendix B is selected as the baseline spectrum $S(\omega, \zeta_0 = 0.05; a_g^s)$, while the EI Centro wave of SOOE (NS) component of the Imperial Valley earthquake on May 18, 1940 is utilized as the seismic record $\ddot{x}_g^R(t)$, shown in Fig. 2(a). Following the procedure outlined in Ref. [37] and summarized in Appendix A for completeness, the EC8 compatible excitation EPS $G(\omega, \zeta_0, t; a_g^s)$ is derived and presented in Fig. 2(b).

A joint time–frequency analysis of the recorded ground motion is carried out by means of the continuous wavelet transform (CWT), which is well suited for transient, nonstationary signals such as seismic excitations. The wavelet coefficients obtained from the CWT serve as the basis for computing the non-separable $G^R(\omega, \zeta_0, t; a_g^s)$ power spectrum component of the seismic record in Eq. (A.12). The resulting excitation EPS $G(\omega, \zeta_0, t; a_g^s)$, compatible with the EC8 design spectrum, is shown in Fig. 2(b) and is employed as the input for the evaluation of bounded time-dependent equivalent linear elements using Eqs. (29) and (30), and subsequently the survival probability over toppling in Eq. (39).

The selected marble blocks, as well as the configurations of the flexible nonlinear foundation models can be found in Refs. [20, 21]. Specifically, two different marble blocks with the following parameter sets were used: Block configuration 1: $2h = 0.42$ m, $2b = 0.07$ m, and $m = 8.67$ kg; Block configuration 2: $2h = 0.28$ m, $2b = 0.07$ m, and $m = 5.84$ kg. Three different foundation models were selected and are discussed in the following sections. To evaluate the accuracy of the proposed technique in estimating the survival probability, comparisons with relevant MCS data are also performed. In this context, an ensemble of $10,000$

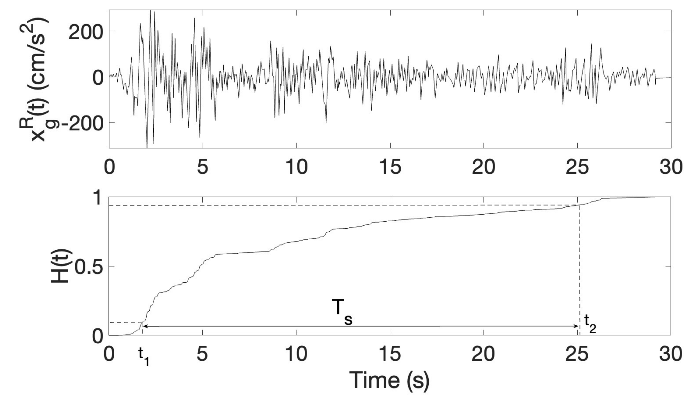

(a)

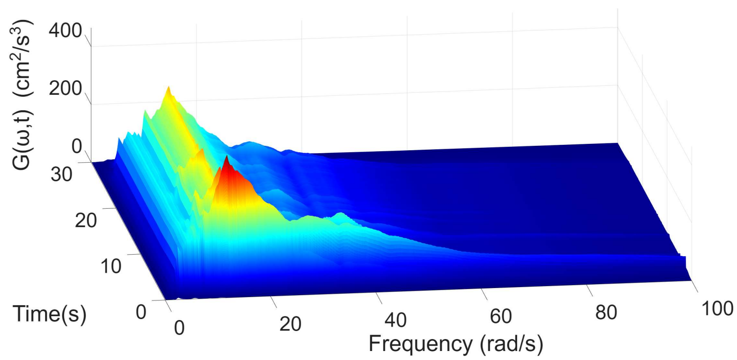

(b)

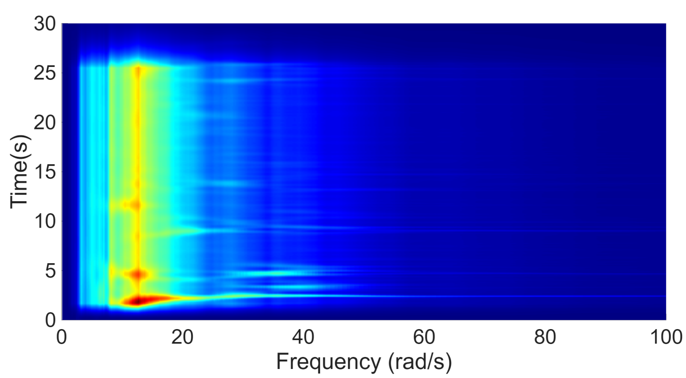

(c)

Fig. 2. (a) Recorded acceleration time-history and associated Husid function of El Centro 1940 earthquake record. Excitation EC8 design spectrum $S(\omega, \zeta_0 = 0.05; a_g^s)$ compatible nonstationary power spectrum for PGA 0.35g: (b) three-dimensional representation, and (c) corresponding top-view projection.

acceleration time histories is generated to align with the EC8 design spectrum, as specified in Eq. (A.11) of Appendix A. Furthermore, Eq. (10), which governs the system dynamics, is numerically integrated for this ensemble, and the survival probability over toppling estimate is derived through statistical analysis of the block rocking response time-histories.

3.1. Block configurations on nonlinear flexible foundation model of type A

The coupled nonlinear equations governing the dynamics of the rocking block system in question are given by Eqs. (1) and (2). Following the static condensation method, the uncoupled equation of block rocking on nonlinear foundation, first, takes the form in Eq. (10). Then, applying the linearization scheme in Section 2.2, Eq. (17) and Eq. (26) are derived, where the bounded equivalent time-dependent damping and stiffness elements are found by Eqs. (29) and (30), respectively. The parameter values for the type A foundation model are $k = 2.89 \times 10^7$ and $\lambda = 8.95 \times 10^8$. Next, a standard integration scheme is used to solve numerically Eq. (33) for determining the coefficient $c(t)$. This is used in conjunction with Eq. (31), and Eqs. (29) and (30) to compute the nonstationary response amplitude PDF and the bounded equivalent linear elements of the system. The latter are shown in Fig. 3 for Block configuration 1 with $PGA = 0.45g$, where a decreasing with time trend is noted. An analogous behavior is observed in the amplitude-dependent equivalent elements. Subsequently, discretizing the time domain as discussed in step (iv.) of Section 2.4, Eqs. (43) and (47) are used to compute H_{i-1} and Q_{i-1}. The latter are then substituted in Eq. (39) to compute the survival probability over toppling P_B. The results obtained for this Block configuration with respect to various values of PGA are shown in Fig. 4, where MCS data are also provided for comparison. Specifically, $10,000$ excitation samples compatible with the reference response spectrum of Eq. (A.12), corresponding to a given PGA level, were generated using the spectral representation method [39]. The governing rocking dynamics, Eqs. (10-13), were then solved by means of a Runge-Kutta numerical integration scheme to obtain the response realizations. Similarly, the survival probabilities against toppling P_B are plotted in Fig. 5 for Block configuration 2. The excitation levels considered for the second block configuration are $0.55g$, $0.65g$, and $0.75g$. These ground-motion levels were deliberately selected because Block configurations 1 and 2 share the same base width $2b$, while the configuration 2 has a significantly lower height $2h$. This geometric difference results in a higher slenderness ratio for configuration 1, making configuration 2 inherently more stable and therefore requiring stronger excitations to overturn; the critical rocking angles are $\theta_{cr,1} = 9.46°$ and $\theta_{cr,2} = 14.00°$, respectively [20]. By subjecting configuration 2 to higher excitation levels, the analyses provide a balanced comparison of the survival probabilities and highlight the robustness of the proposed methodology across blocks with varying geometrical proportions. The proposed approximate technique shows a satisfactory degree of accuracy.

3.2. Block configurations on nonlinear flexible foundation model of type B

Considering next the foundation model of type B with parameter values $k = 6.88 \times 10^6$ and $\lambda = 1.3 \times 10^8$, the survival probabilities over toppling P_B of

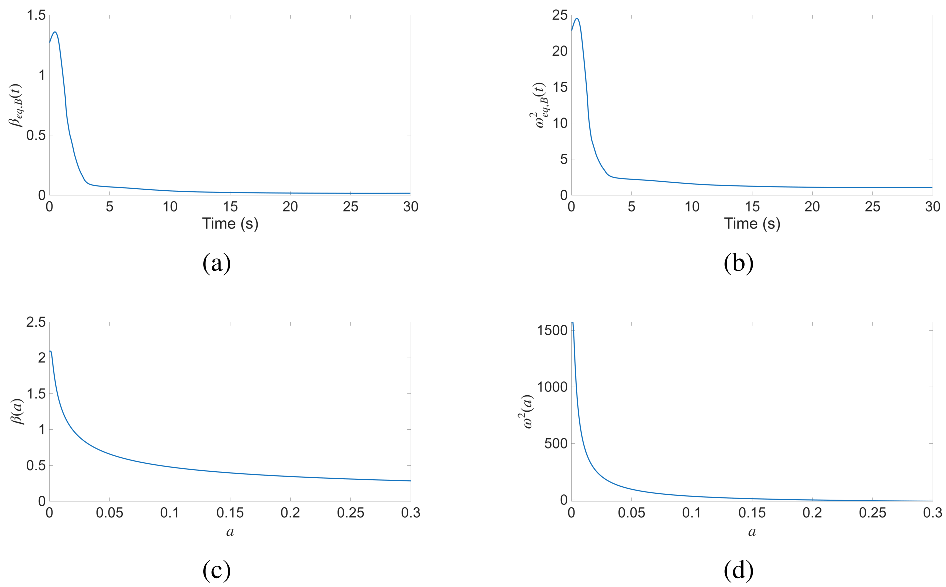

Fig. 3. Bounded time-dependent equivalent elements (Block configuration 1): (a) damping $\beta_{eq,B}(t)$; (b) stiffness $\omega^2_{eq,B}(t)$; and amplitude-dependent equivalent elements: (c) damping $\beta(a)$; (d) stiffness $\omega^2(a)$ for the rigid block rocking on nonlinear flexible foundation of Type A under evolutionary seismic excitation.

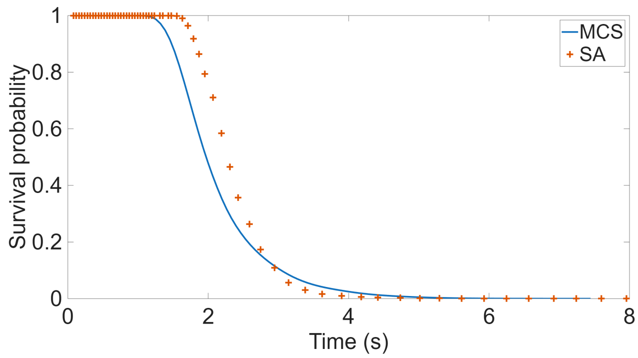

(a)

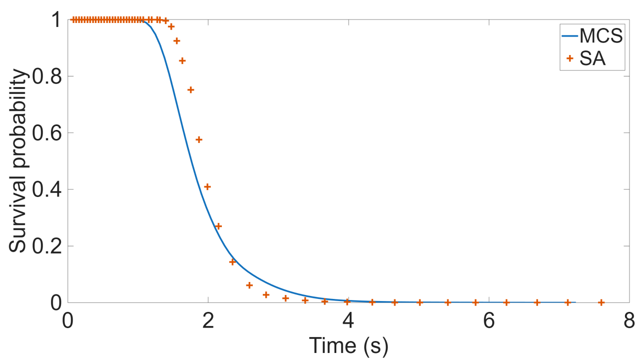

(b)

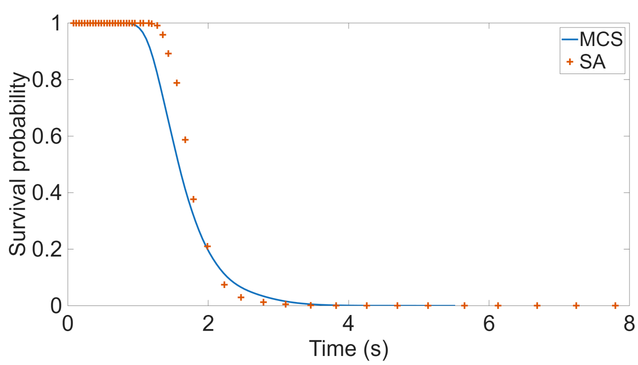

(c)

Fig. 4. Toppling survival probability estimates obtained via the proposed stochastic averaging-based (SA) method and Monte Carlo simulation (MCS) for a rigid block (Block configuration 1) rocking on a flexible foundation (Type A model), subjected to evolutionary nonstationary seismic excitation compatible with EC8 specifications: (a) $PGA = 0.45g$; (b) $PGA = 0.55g$; (c) $PGA = 0.65g$.

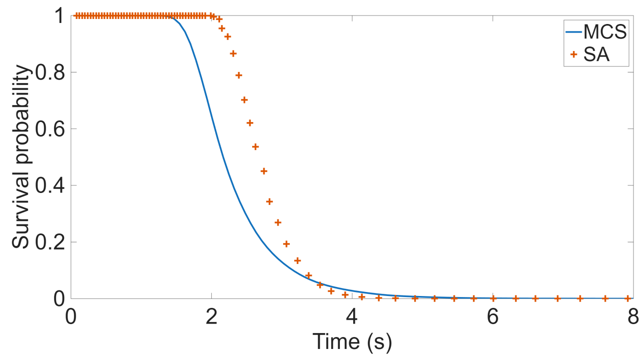

(a)

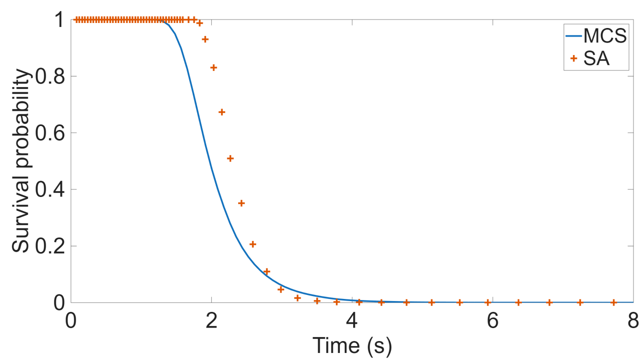

(b)

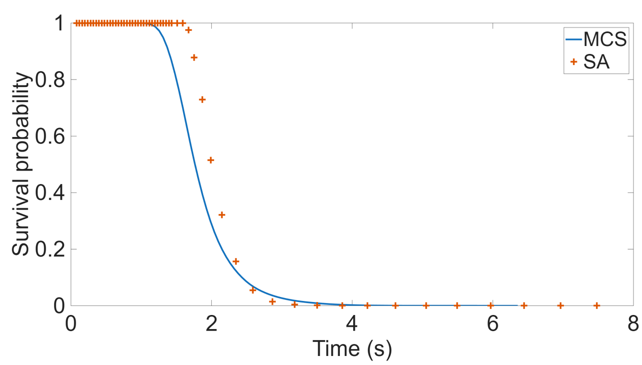

(c)

Fig. 5. Toppling survival probability estimates obtained via the proposed stochastic averaging-based (SA) method and Monte Carlo simulation (MCS) for a rigid block (Block configuration 2) rocking on a flexible foundation (Type A model), subjected to evolutionary nonstationary seismic excitation compatible with EC8 specifications: (a) $PGA = 0.55g$; (b) $PGA = 0.65g$; (c) $PGA = 0.75g$.

Block configurations 1 and 2 are efficiently determined following the presentation in Section 2.4, and plotted in Figs. 6 and 7, respectively, for the corresponding ranges of PGA values. Similar to Section 3.1, comparisons with pertinent MCS data, including $10,000$ samples, demonstrate a satisfactory degree of accuracy. At higher levels of ground motion excitation, the systems exhibit a rapid decline in survival probability, with overturning occurring at earlier time instances.

3.3. Block configurations on nonlinear flexible foundation model of type C

In this case, the foundation model of type C characterized by the parameters $k = 6.42 \times 10^6$ and $\lambda = 1.65 \times 10^8$ is considered. The survival probabilities over toppling P_B of Block configurations 1 and 2 are computed as described in Section 2.4 and illustrated in Figs. 8 and 9, respectively, for the corresponding ranges of PGA values. In both figures, the results are compared with MCS data comprising $10,000$ samples, revealing a satisfactory level of accuracy.

4. Concluding remarks

A novel semi-analytical approximate framework is proposed in this paper to assess the toppling survival probability of rigid block systems rocking under stochastic ground motion. The proposed framework incorporates a nonlinear flexible foundation model that allows for uplifting and nonlinear damping, reflecting realistic soil-structure interaction effects. Formulating a special nonstationary probability density function for the rocking amplitude, the method demonstrates its capability to effectively manage nonstationary seismic excitation loading, accurately capturing the fluctuations in intensity and frequency content of real seismic

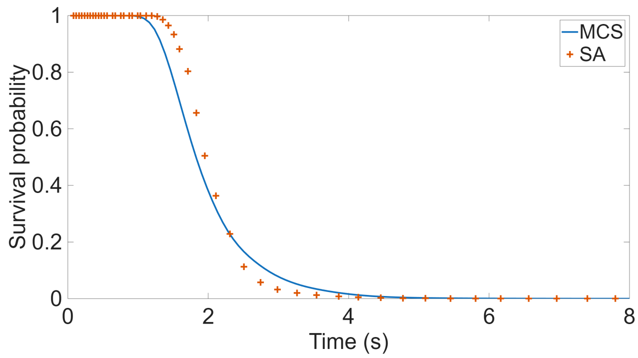

(a)

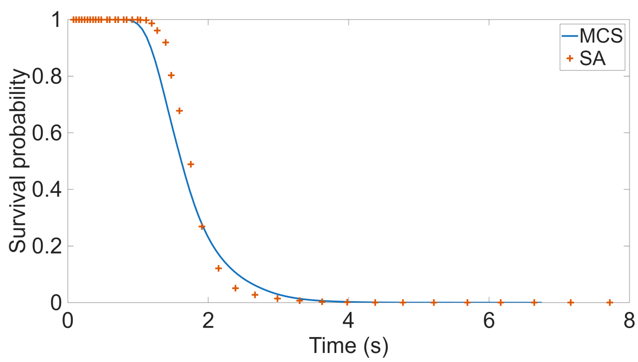

(b)

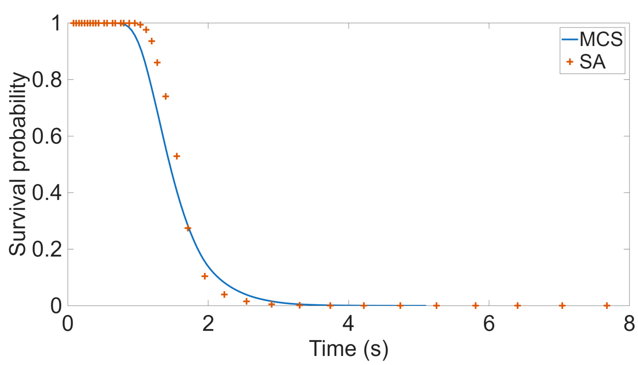

(c)

Fig. 6. Toppling survival probability estimates obtained via the proposed stochastic averaging-based (SA) method and Monte Carlo simulation (MCS) for a rigid block (Block configuration 1) rocking on a flexible foundation (Type B model), subjected to evolutionary nonstationary seismic excitation compatible with EC8 specifications: (a) $PGA = 0.45g$; (b) $PGA = 0.55g$; (c) $PGA = 0.65g$.

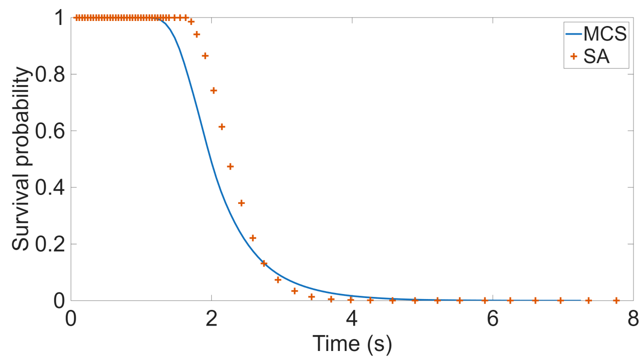

(a)

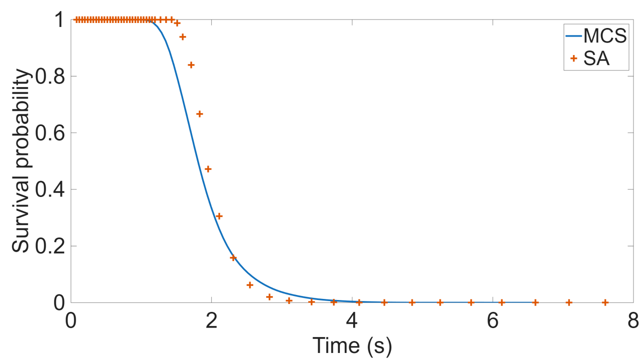

(b)

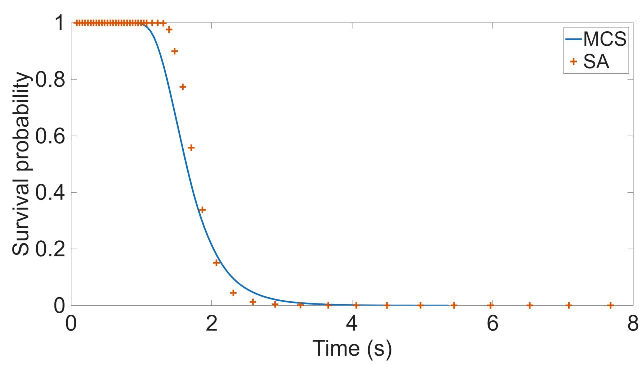

(c)

Fig. 7. Toppling survival probability estimates obtained via the proposed stochastic averaging-based (SA) method and Monte Carlo simulation (MCS) for a rigid block (Block configuration 2) rocking on a flexible foundation (Type B model), subjected to evolutionary nonstationary seismic excitation compatible with EC8 specifications: (a) $PGA = 0.55g$; (b) $PGA = 0.65g$; (c) $PGA = 0.75g$.

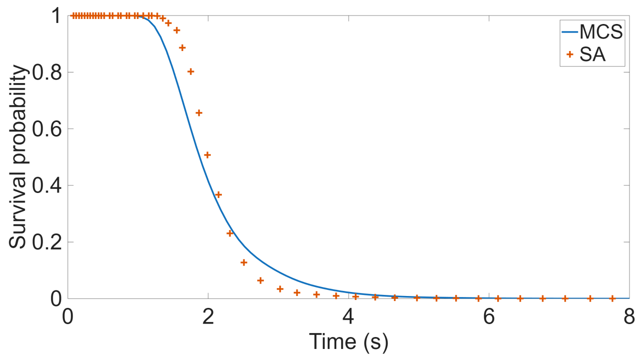

(a)

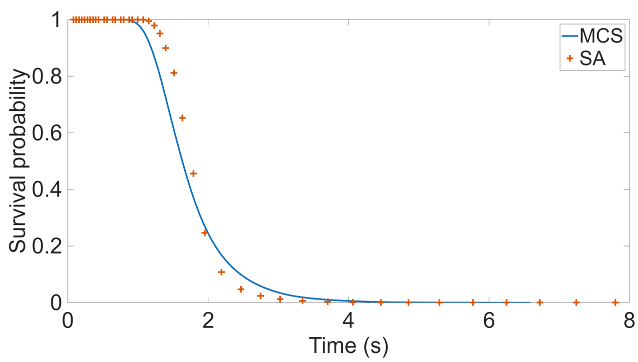

(b)

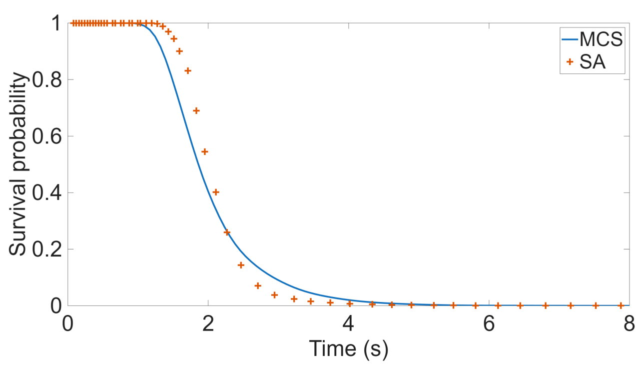

(c)

Fig. 8. Toppling survival probability estimates obtained via the proposed stochastic averaging-based (SA) method and Monte Carlo simulation (MCS) for a rigid block (Block configuration 1) rocking on a flexible foundation (Type C model), subjected to evolutionary nonstationary seismic excitation compatible with EC8 specifications: (a) $PGA = 0.45g$; (b) $PGA = 0.55g$; (c) $PGA = 0.65g$.

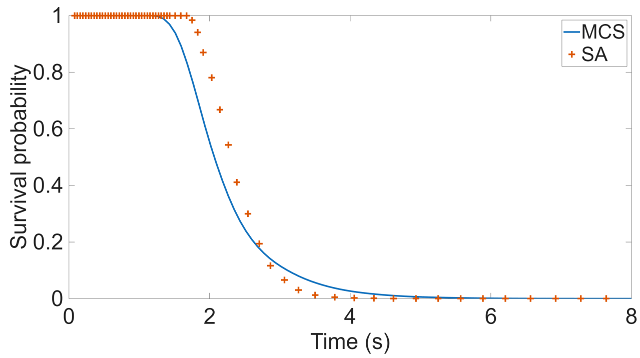

(a)

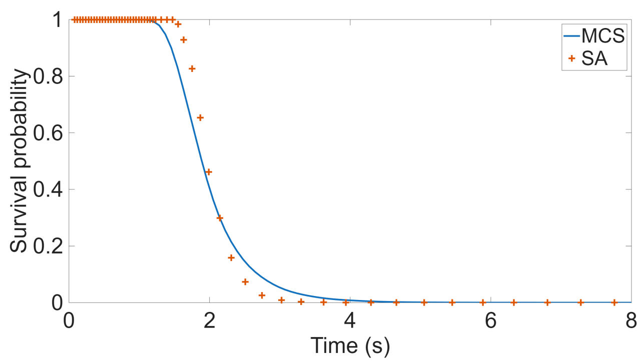

(b)

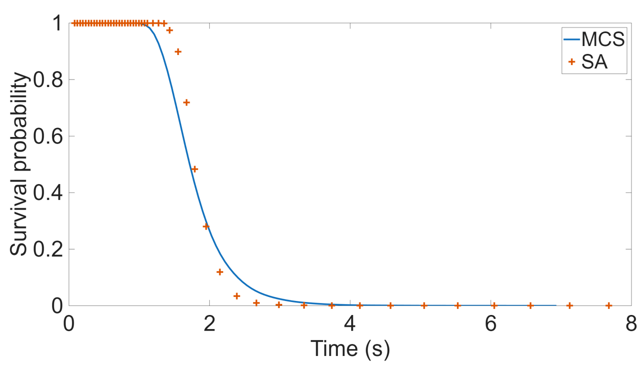

(c)

Fig. 9. Toppling survival probability estimates obtained via the proposed stochastic averaging-based (SA) method and Monte Carlo simulation (MCS) for a rigid block (Block configuration 2) rocking on a flexible foundation (Type C model), subjected to evolutionary nonstationary seismic excitation compatible with EC8 specifications: (a) $PGA = 0.55g$; (b) $PGA = 0.65g$; (c) $PGA = 0.75g$.

events. The proposed framework showcases considerable computational advantages compared to traditional approaches, facilitating the efficient quantification of survival probabilities over toppling. Additionally, a notable advancement pertains to its capacity to incorporate unbounded response behaviors associated with negative values of stiffness, thus addressing a significant gap in the literature. The accuracy and reliability of the proposed framework are validated through relevant numerical examples, and comparisons with Monte Carlo simulation data reveal its applicability in evaluating the performance of rigid blocks rocking on nonlinear foundations under non-white seismic loading. The proposed framework advances the theoretical understanding of nonlinear rocking block dynamics and holds practical significance for potential engineering applications aligned with modern resilience-oriented seismic perspectives.

Declaration of competing interest

The authors declare that they have no known competing financial interests or personal relationships that could have appeared to influence the work reported in this paper.

Acknowledgment

The authors gratefully acknowledge the support by the Hellenic Foundation for Research and Innovation (Grant No. 1261).

Appendix A. Derivation of Design Spectrum-Compatible Nonstationary Power Spectra

Based on the approach proposed by Cacciola in Ref. [37], the nonstationary stochastic ground acceleration $\ddot{x}_g(t)$ is expressed in the form

$$\ddot{x}_g(t) = \alpha \ddot{x}_g^R(t) + \psi(t)\ddot{x}_g^S(t), \tag{A.1}$$

where $\ddot{x}_g^R(t)$ denotes a fully nonstationary segment extracted from an actual seismic record, α is a spectral scaling factor, and $\ddot{x}_g^S(t)$ represents a quasi-stationary Gaussian corrective process, modulated in time by $\psi(t)$. The time-modulating function $\psi(t)$ follows the formulation proposed by Jennings [40]

$$\psi(t) = \begin{cases} \left(\frac{t}{t_1}\right)^2, & t < t_1 \\ 1, & t_1 \leq t \leq t_2 \\ \exp[-\beta_m(t - t_2)], & t > t_2 \end{cases} \tag{A.2}$$

where t_1 and t_2 are defined such that the Husid function [41] attains 5% and 95% of its maximum, respectively, with $T_s = t_2 - t_1$ denoting the stationary phase duration. The parameter β_m governs the decay rate.

For a linear SDOF system subjected to $\ddot{x}_g^R(t)$ and $\ddot{x}_g^S(t)$ with respective response spectra $S^R(\omega, \zeta_0; a_g^s)$ and $S^S(\omega, \zeta_0; a_g^s)$, the combined target response spectrum takes the form

$$S(\omega, \zeta_0; a_g^s) = \sqrt{\alpha^2 S^R(\omega, \zeta_0; a_g^s)^2 + S^S(\omega, \zeta_0; a_g^s)^2}, \tag{A.3}$$

with $\alpha \in (0, 1]$ selected as

$$\alpha = \min \left\{ \frac{S(\omega, \zeta_0; a_g^s)}{S^R(\omega, \zeta_0; a_g^s)} \right\}. \tag{A.4}$$

To derive the spectral density that integrates first-passage approximations [42] and iterative refinement [43] is employed next. The pseudo-acceleration spectrum is linked to the spectral moments via

$$S^S(\omega_0, \zeta_0; a_g^s) = \eta_{x^S} \omega_0^2 \sqrt{\lambda_{0,x^S}(\omega_0, \zeta_0; a_g^s)}, \tag{A.5}$$

where λ_{n,x^S} denotes the nth-order spectral moment

$$\lambda_{n,x^S}(\omega_0, \zeta_0; a_g^s) = \int_0^\infty \omega^n \frac{G^S(\omega, \zeta_0; a_g^s)}{(\omega_0^2 - \omega^2)^2 + (2\zeta_0\omega_0\omega)^2} \mathrm{d}\omega \tag{A.6}$$

and η_{x^S} accounts for the peak factor, given by [42]

$$\eta_{x^S}(T_s, p) = \sqrt{2 \ln \left(2\mu_{x^S} \left[1 - \exp \left(-\delta_{x^S}^{1.2} \sqrt{\pi \ln(2\mu_{x^S})} \right) \right] \right)}, \tag{A.7}$$

with

$$\mu_{x^S} = \frac{T_s}{2\pi} \sqrt{\frac{\lambda_{2,x^S}}{\lambda_{0,x^S}}} (-\ln p)^{-1}, \quad \delta_{x^S} = \sqrt{1 - \frac{\lambda_{1,x^S}^2}{\lambda_{0,x^S}\lambda_{2,x^S}}}. \tag{A.8}$$

Setting $p = 0.5$ and applying a closed-form approximation [42], Eq. (A.5) becomes

$$S^S(\omega_0, \zeta_0; a_g^s) = \eta_{x^S}^2 \omega_0 G^S(\omega_0, \zeta_0; a_g^s) \left(\frac{\pi - 4\zeta_0}{4\zeta_0} \right) + \eta_{x^S}^2 \int_0^{\omega_0} G^S(\omega, \zeta_0; a_g^s) \, \mathrm{d}\omega. \tag{A.9}$$

Next, discretizing the frequency domain into N intervals with $\omega_i = \omega_l + (i - 0.5)\Delta\omega$, $i = 1, 2, ..., N$, yields

$$G^S(\omega_i, \zeta_0; a_g^s) = \begin{cases} 0, & \omega_i \leq \omega_l \\ \frac{4\zeta_0}{\pi\omega_i - 4\zeta_0\omega_{i-1}} \left(\frac{S^S(\omega_i, \zeta_0; a_g^s)^2}{\eta_{x^S}^2} \right. & \\ \qquad \left. - \Delta\omega \sum_{k=1}^{i-1} G^S(\omega_k, \zeta_0; a_g^s) \right), & \omega_l < \omega_i < \omega_u \end{cases} \tag{A.10}$$

which is applied recursively. Once $G^S(\omega, \zeta_0; a_g^s)$ is determined, the spectral representation method [39] is employed to generate realizations of the corrective acceleration process

$$\ddot{x}_g^{(j)}(t) = \alpha \ddot{x}_g^R(t) + \psi(t) \sum_{i=1}^{N_a} \sqrt{4G^S(i\Delta\omega, \zeta_0; a_g^s)\Delta\omega} \cos(i\Delta\omega t + \theta_i^{(j)}), \tag{A.11}$$

where $\theta_i^{(j)}$ are independent random phases uniformly distributed in $[0, 2\pi)$.

The resulting evolutionary power spectral density (EPSD) for $\ddot{x}_g(t)$ becomes

$$G(\omega, \zeta_0, t; a_g^s) = \alpha^2 G^R(\omega, \zeta_0, t; a_g^s) + \psi(t)^2 G^S(\omega, \zeta_0; a_g^s), \tag{A.12}$$

where $G^R(\omega, \zeta_0, t; a_g^s)$ and $G^S(\omega, \zeta_0; a_g^s)$ denote the non-separable and separable EPSD components, respectively [44–46].

Finally, to improve spectral matching, the iterative scheme

$$G^{S(k)}(\omega, \zeta_0; a_g^s) = G^{S(k-1)}(\omega, \zeta_0; a_g^s) \left[\frac{S(\omega, \zeta_0; a_g^s)^2}{\tilde{S}^{(k-1)}(\omega, \zeta_0; a_g^s)^2} \right] \tag{A.13}$$

is used, where $\tilde{S}^{(k)}(\omega, \zeta_0; a_g^s)$ denotes the mean response spectrum generated from the kth iteration.

Appendix B. Eurocode 8 design spectrum

The Eurocode 8 defines the elastic pseudo-acceleration response spectrum for linear oscillators with damping ratio ζ and natural period $T = 2\pi/\omega$ through the following relationships [47]

$$S(T, \zeta) = a_g^0 \times \begin{cases} S\left[1 + \frac{T}{T_B}(2.5\eta - 1)\right], & 0 \leq T \leq T_B \\ 2.5S\eta, & T_B \leq T \leq T_C \\ 2.5S\eta\frac{T_C}{T}, & T_C \leq T \leq T_D \\ 2.5S\eta\frac{T_C T_D}{T^2}, & T_D \leq T \leq T_E \\ S\frac{T_C T_D}{T^2}\left[2.5\eta + \frac{T - T_E}{T_F - T_E}(1 - 2.5\eta)\right], & T_E \leq T \leq T_F \\ S\frac{T_C T_D}{T^2}, & T_F \leq T \end{cases}, \tag{B.1}$$

where

$$\eta = \sqrt{\frac{10}{5 + \zeta}} \geq 0.55, \tag{B.2}$$

with a_g^0 denoting the peak ground acceleration, S denoting a soil-dependent amplification factor, and T_B, T_C, T_D, T_E and T_F corresponding to soil-dependent corner periods. The set of parameter values used for soil type B are $S = 1.20$,

$T_B = 0.15$, $T_C = 0.5$, $T_D = 2.0$, $T_E = 5.0$, and $T_F = 10$.

References

[1] G. W. Housner, The behavior of inverted pendulum structures during earthquakes, Bulletin of the Seismological Society of America 53 (1963) 403–417.

[2] I. N. Psycharis, P. C. Jennings, Rocking of slender rigid bodies allowed to uplift, Earthquake Engineering and Structural Dynamics 11 (1983) 57–76.

[3] A. S. Koh, P. D. Spanos, J. M. Roesset, Harmonic rocking of rigid block on flexible foundation, Journal of Engineering Mechanics 112 (11) (1986) 1165–1180.

[4] A. Palmeri, N. Makris, Response analysis of rigid structures rocking on viscoelastic foundation, Earthquake Engineering and Structural Dynamics 37 (2008) 1039–1063.

[5] M. N. Chatzis, A. W. Smyth, Robust modeling of the rocking problem, Journal of Engineering Mechanics 138 (2012) 247–262.

[6] P. A. Bońkowski, Z. Zembaty, M. Y. Minch, Engineering analysis of strong ground rocking and its effect on tall structures, Soil Dynamics and Earthquake Engineering 116 (2019) 358–370.

[7] N. Makris, M. F. Vassiliou, Sizing the slenderness of free-standing rocking

columns to withstand earthquake shaking, Archive of Applied Mechanics 82 (2012) 1497–1511.

[8] L. Gioiella, E. Tubaldi, F. Gara, L. Dezi, A. Dall'Asta, Modal properties and seismic behaviour of buildings equipped with external dissipative pinned rocking braced frames, Engineering Structures 172 (2018) 807–819.

[9] D. Konstantinidis, N. Makris, Experimental and analytical studies on the response of freestanding laboratory equipment to earthquake shaking, Earthquake Engineering and Structural Dynamics 38 (2009) 827–848.

[10] A. N. Kounadis, Seismic instability of free-standing statues atop multispondyle columns: A heuristic very stable system of ancient technology, Soil Dynamics and Earthquake Engineering 119 (2019) 253–264.

[11] M. Dimentberg, Y. Lin, R. Zhang, Toppling of computer-type equipment under base excitation, Journal of engineering mechanics 119 (1) (1993) 145–160.

[12] A. Di Matteo, A. Pirrotta, E. Gebel, P. D. Spanos, Analysis of block random rocking on nonlinear flexible foundation, Probabilistic Engineering Mechanics 59 (2020) 103017.

[13] R. Iyengar, C. Manohar, Rocking response of rectangular rigid blocks under random noise base excitations, International journal of non-linear mechanics 26 (6) (1991) 885–892.

[14] H. Lin, S. Yim, Nonlinear rocking motions. ii: Overturning under random excitations, Journal of engineering mechanics 122 (8) (1996) 728–735.

[15] I. P. Mitseas, I. A. Kougioumtzoglou, P. D. Spanos, M. Beer, Nonlinear MDOF structural system survival probability determination subject to evolutionary stochastic excitation, Strojniski Vestnik-Journal of Mechanical Engineering 62 (7-8) (2016) 440–451.

[16] I. A. Kougioumtzoglou, Y. Zhang, M. Beer, Softening duffing oscillator reliability assessment subject to evolutionary stochastic excitation, ASCE-ASME Journal of Risk and Uncertainty in Engineering Systems, Part A: Civil Engineering 2 (2) (2015) 04015002.

[17] I. P. Mitseas, P. Ni, V. C. Fragkoulis, M. Beer, Survival probability surfaces of hysteretic fractional order structures exposed to non-stationary code-compliant stochastic seismic excitation, Engineering Structures 318 (2024) 118755.

[18] I. A. Kougioumtzoglou, P. Ni, I. P. Mitseas, V. C. Fragkoulis, M. Beer, An approximate stochastic dynamics approach for design spectrum-based response analysis of nonlinear oscillators with fractional derivative elements, International Journal of Non-Linear Mechanics 146 (2022) 104178.

[19] D. Jerez, V. Fragkoulis, P. Ni, I. Mitseas, M. A. Valdebenito, M. G. Faes, M. Beer, Operator norm-based determination of failure probability of nonlinear oscillators with fractional derivative elements subject to imprecise

stationary gaussian loads, Mechanical Systems and Signal Processing 208 (2024) 111043.

[20] P. D. Spanos, A. Di Matteo, A. Pirrotta, M. Di Paola, Rocking of rigid block on nonlinear flexible foundation, International Journal of Non-Linear Mechanics 94 (2017) 362–374.

[21] A. D. Matteo, A. Pirrotta, E. Gebel, P. D. Spanos, Analysis of block random rocking on nonlinear flexible foundation, Probabilistic Engineering Mechanics 59 (2020) 103017.

[22] A.-S. Koh, Rocking of rigid blocks on randomly shaking foundations, Nuclear Engineering and Design 97 (1986) 269–276.

[23] K. H. Hunt, F. R. E. Crossley, Coefficient of restitution interpreted as damping in vibroimpact, Journal of Applied Mechanics 42 (2) (1975) 440–445.

[24] G. Gilardi, I. Sharf, Literature survey of contact dynamics modelling, Mechanism and Machine Theory 37 (10) (2002) 1213–1239.

[25] P. Frost, P. Cacciola, Rocking of rigid non-symmetric blocks standing on a horizontally-moving compliant base, Engineering Structures 312 (2024) 118245.

[26] P. Frost, P. Cacciola, Dynamic cross-interaction between two adjacent rocking blocks, Soil Dynamics and Earthquake Engineering 178 (2024) 108483.

[27] I. A. Kougioumtzoglou, P. D. Spanos, An approximate approach for nonlinear system response determination under evolutionary stochastic excitation, Current science (2009) 1203–1211.

[28] P.-T. D. Spanos, L. D. Lutes, Probability of response to evolutionary process, Journal of the Engineering Mechanics Division 106 (2) (1980) 213–224.

[29] J. B. Roberts, P. D. Spanos, Random vibration and statistical linearization, Courier Corporation, 2003.

[30] P. D. Spanos, I. A. Kougioumtzoglou, Survival probability determination of nonlinear oscillators subject to evolutionary stochastic excitation, Journal of Applied Mechanics 81 (5) (2014) 051016.

[31] I. P. Mitseas, M. Beer, Modal decomposition method for response spectrum based analysis of nonlinear and non-classically damped systems, Mechanical Systems and Signal Processing 131 (2019) 469–485.

[32] I. A. Kougioumtzoglou, P. D. Spanos, Stochastic response analysis of the softening duffing oscillator and ship capsizing probability determination via a numerical path integral approach, Probabilistic Engineering Mechanics 35 (2014) 67–74.

[33] J. B. Roberts, P. D. Spanos, Stochastic averaging: an approximate method of solving random vibration problems, International Journal of Non-Linear Mechanics 21 (2) (1986) 111–134.

[34] W. Q. Zhu, Stochastic averaging methods in random vibration, Applied Mechanics Reviews 41 (5) (1988) 189–199.

[35] P. D. Spanos, G. P. Solomos, Markov approximation to transient vibration, Journal of Engineering Mechanics 109 (4) (1983) 1134–1150.

[36] I. P. Mitseas, M. Beer, First-excursion stochastic incremental dynamics methodology for hysteretic structural systems subject to seismic excitation, Computers & Structures 242 (2021) 106359.

[37] P. Cacciola, A stochastic approach for generating spectrum compatible fully nonstationary earthquakes, Computers & Structures 88 (15-16) (2010) 889–901.

[38] P. Ni, I. P. Mitseas, V. C. Fragkoulis, M. Beer, Spectral incremental dynamic methodology for nonlinear structural systems endowed with fractional derivative elements subjected to fully non-stationary stochastic excitation, Structural Safety 111 (2024) 102525.

[39] M. Shinozuka, G. Deodatis, Simulation of stochastic processes by spectral representation, ASME. Appl. Mech. Rev. 44 (4) (1995) 191–204.

[40] P. C. Jennings, Equivalent viscous damping for yielding structures, Journal of the Engineering Mechanics Division 94 (1) (1968) 103–116.

[41] R. L. Husid, Analisis de terremotos – analisis general, Revista del IDEM 8 (1969) 21–42.

[42] E. H. Vanmarcke, Structural response to earthquakes, in: Developments in Geotechnical Engineering, Vol. 15, Elsevier, 1976, pp. 287–337.

[43] P. Cacciola, P. Colajanni, G. Muscolino, Combination of modal responses consistent with seismic input representation, Journal of Structural Engineering 130 (1) (2004) 47–55.

[44] L. Cohen, Time-frequency distributions-a review, Proceedings of the IEEE 77 (7) (1989) 941–981.

[45] J. P. Conte, B.-F. Peng, An explicit closed-form solution for linear systems subjected to nonstationary random excitation, Probabilistic Engineering Mechanics 11 (1) (1996) 37–50.

[46] P. D. Spanos, G. Failla, Evolutionary spectra estimation using wavelets, Journal of Engineering Mechanics 130 (8) (2004) 952–960.

[47] CEN, Eurocode 8: Design of Structures for Earthquake Resistance - Part 1: General Rules, Seismic Actions and Rules for Buildings, Comité Européen de Normalisation, Brussels EN 1998-1: 2003 E. (2004).